Eur. Phys. J. B **44**, 3–14 (2005)
DOI: 10.1140/epjb/e2005-00093-7

THE EUROPEAN PHYSICAL JOURNAL B

Depolarized light scattering study of glycerol

A. Brodin[a] and E.A. Rössler[b]

Experimentalphysik II, Universität Bayreuth, 95440 Bayreuth, Germany

Received 22 October 2004
Published online 16 April 2005 –

Abstract. We have obtained depolarized (anisotropic) light scattering spectra of the glass forming material glycerol in a wide temperature (160 to 430 K) and frequency (0.4 GHz to 48 THz) range and compared them with light scattering and dielectric spectroscopic data from the literature. The excess wing, which is usually discussed concerning dielectric data, is strongly pronounced in light scattering of glycerol. The temperature evolution of the wing, together with that of the fast relaxation spectrum, leads to a susceptibility minimum that persists in the spectra down to $T_g \approx 185$ K and flattens with decreasing the temperature below ∼290 K. The α-peak in light scattering is significantly wider and weaker in amplitude than in the dielectric loss spectra, and thus cannot be interpolated by the asymptotic laws of the mode coupling theory (MCT). However, similar trends were reported in the literature for solutions of MCT models for rotational dynamics. Furthermore we can identify in both the light scattering and the dielectric data two distinct regimes of temperature evolution with a blurred crossover in the range of 300–320 K. The high-temperature regime is characterized by a nearly temperature independent shape of the α-peak and of the susceptibility minimum, and a nearly temperature independent strength of the fast dynamics. In contrast, at low temperatures the excess wing emerges and the relaxation strength of the fast dynamics changes strongly with the temperature.

PACS. 64.70.Pf Glass transitions – 77.22.Gm Dielectric loss and relaxation – 78.35.+c Brillouin and Rayleigh scattering; other light scattering

1 Introduction

Glycerol is one of the archetypal and most thoroughly studied glassformers. Its relaxation dynamics has been investigated by inelastic neutron scattering, depolarized light scattering, and dielectric spectroscopy, among others. In particular, the broad band dielectric spectra of Lunkenheimer et al. [1], covering the frequency range from μHz to THz at temperatures from 184 K (a few degrees below T_g) up to 413 K, probably comprise the most complete dataset of a glassformer available to date. Other works provided similar results, lacking however data in the THz frequency band [2–5]. The wealth of available physical information thus makes glycerol a particularly good candidate for analyses aimed at understanding similarities and differences between the data obtained by different techniques, and at testing the validity of different phenomenological models and theoretical approaches to the glass transition phenomenon, in particular of the mode coupling theory (MCT) [6]. We mention below some selected investigations with the intention to show that their results concerning comparisons with theoretical predictions are at best confusing. In 1994, Wuttke et al. [7] conducted a parallel incoherent neutron and depolarized light scattering study of glycerol. They observed that the neutron and light spectra were qualitatively similar, although refrained from making more specific conclusions from this comparison. They also analyzed the applicability of MCT and found that their data where moderately compatible with the theory, yielding the critical temperature $T_c = 225$ K. They noted, however, that the viscosity data implied a much higher $T_c = 305$ K, and thus a consistent T_c could not be obtained. Rössler et al. [8] extracted an even higher $T_c = 310$ K from Raman scattering and viscosity data. Two years later Lunkenheimer et al. [9] analyzed dielectric spectra of glycerol and found $T_c = 262$ K, apparently in support of the conclusion of Wuttke et al. that a consistent T_c cannot be obtained. In 1997, Franosch et al. [10] re-analyzed the light scattering data of Wuttke et al., using the so-called two-correlator MCT model, and found a perfect agreement with the theory yielding a T_c between 223 and 233 K. These authors refrained, however, from any comments on alternative estimates of T_c. Yet two years later one of them remarked in his extensive review of experimental tests of MCT that these analyses "did not lead to a compelling estimate of T_c" [11]. Quite recently, Adichtchev et al. [12] analyzed the dielectric data of Lunkenheimer et al. [1], which supersede the earlier dataset of reference [9], and found

[a] e-mail: brodin@romeo.phy.uni-bayreuth.de
[b] e-mail: Ernst.Roessler@uni-bayreuth.de

that the data could be described with MCT asymptotic laws, yielding $T_c = 288$ K. Indeed, it appears impossible to find a consistent T_c, and it is in no way clear whether these discrepancies are due to inapplicability of MCT to glycerol, or rather due to inconsistency of different datasets. Also, apart from Wuttke et al., nobody attempted to quantitatively compare the spectral shapes obtained by different techniques, even though such a comparison would seem a natural initial step before an MCT analysis, as the theory makes specific predictions in this respect, though qualitative comparisons were reported [1,7]. One has however to note that such comparisons of dielectric data at high (THz) frequencies, i.e. in the range of fast relaxations and the boson peak, were not possible until recently, when the broad band spectra became available, and even then only for glycerol and propylene carbonate [1]. As for the data consistency, the dielectric data of references [1,4,5] are in close agreement with each other and appear to be the most accurate to date. However, the accuracy of the light and neutron scattering data of Wuttke et al. is not known. Moreover, there are reasons to believe that their light scattering spectra, which were obtained using a tandem Fabry-Perot interferometer, may contain artifacts due to the overlap of different interference orders (spectral folding), a problem that was not recognized until a few years later [13,14].

We have undertaken the present study in an attempt to resolve some of the mentioned discrepancies. We obtained a new set of depolarized light scattering spectra of glycerol in a wide temperature (160 to 430 K) and frequency (0.4 GHz to 48 THz) range, taking the necessary precautions to avoid instrumental artefacts. For comparisons, we also obtained a few depolarized light scattering spectra of propylene carbonate, which is another classical glassformer. We then analyzed these data and compared them with the dielectric results of Lunkenheimer et al., attempting to i) shed more light on the relation between dielectric and light scattering spectra of molecular liquids, ii) separate universal features of the susceptibility spectra from method-dependent ones, and iii) see whether a consistent MCT analysis is possible.

2 Experimental

Glycerol ($C_3H_5(OH)_3$) is a trihydric alcohol that forms a week hydrogen-bond network. Its boiling point $T_b \approx 565$ K is thereby rather high; by contrast, alkanes with similar molecular weights, hexane and heptane, boil at 342 and 371 K, respectively. It supercools easily below $T_m = 291$ K and forms a glass at $T_g \simeq 185$ K. Samples of glycerol where contained in 15 mm diameter crimp-capped glass vials [15] and in rectangular 10 mm optical glass cells. In the latter case, we filled the cells under nitrogen with spectroscopic grade glycerol (Aldrich, 99.5+%) and sealed them with teflon plugs. All samples that we tested produced nearly indistinguishable depolarized spectra. The only difference was the optical quality of the cells, notably their optical anisotropy. A sample cell was mounted either in an optical continuous-flow LHe cryostat (CryoVac) for measurements below room temperature, or in a home-built mini-furnace. Two calibrated Si-diode temperature sensors where mounted in the cryostat, and a Pt100 platinum resistance thermometer in the furnace. The accuracy of the temperature reading is believed to be better than 0.1 K and 0.2 K for the Si-diodes and platinum resistance, respectively. A LakeShore temperature controller was used for temperature regulation. The sample was illuminated by a ∼170 mW 532 nm horizontally-polarized laser beam from a Coherent Verdi V2 frequency-doubled Nd:YVO_4 single mode laser. Two collection paths of scattered radiation were used simultaneously. Firstly, vertically polarized light scattered at $\simeq 174°$ with respect to the excitation beam was fed into a multipath tandem Fabry-Perot scanning interferometer equipped with a low noise avalanche diode (JRS Scientific Instruments), thus employing HV (horizontal-vertical, depolarized) nearly-backscattering geometry. Secondly, light scattered at 90° was directed, without polarization selection, into a U1000 (Jobin Yvon) double grating monochromator, thus utilizing 90° HT (horizontal-total, depolarized) scattering configuration. At each temperature, partial spectra were collected over several overlapping spectral ranges with different settings of the instruments. Interferometric spectra were accumulated using free spectral ranges (FSR) of 15, 75, 150, and 300 GHz, typically for one to several hours at each instrument setting. The spectra were then corrected for the instrumental spectral response that was measured separately for each FSR using a white light source. Finally, the partial spectra were divided by the appropriate Bose factors and spliced to form composite spectra spanning 5 decades in frequency, see Figure 1. In order to circumvent the "spectral folding" effect, whereby spurious additional intensity appears in the working interference order because of the transmission in other orders, we used additional narrow-band filters to limit the total bandwidth. One of the filters with FWHM of 200 GHz or 1 THz (Andover Corporation) was used, depending on FSR. We estimate that suppression of additional orders was in most cases better than 10^3; in the worst case (200 GHz filter, 15 GHz FSR) the nearest orders at $\pm 20\times$ FSR were reduced by at least 10^2.

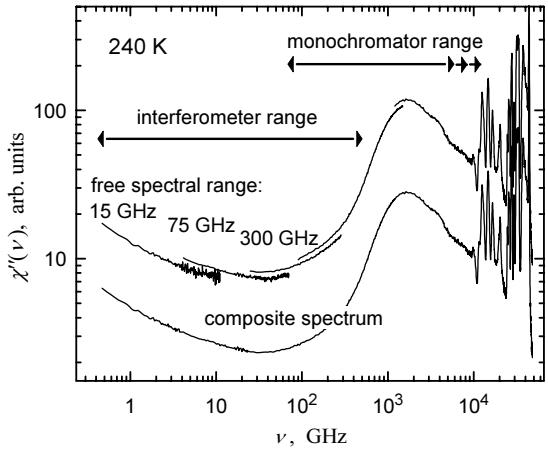

Fig. 1. Splicing partial interferometer and monochromator spectra.

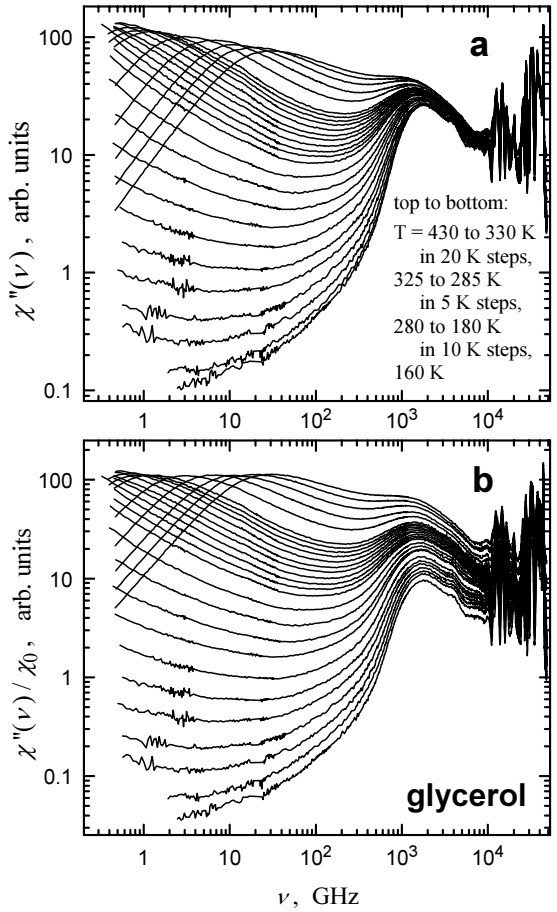

Fig. 2. (a) Depolarized (anisotropic) light scattering susceptibility spectra of glycerol at indicated temperatures. (b) The same spectra divided by the temperature-dependent static susceptibility (Sect. 3.2 and Fig. 5).

3 Results and discussion

Figure 2a presents depolarized light scattering spectra of glycerol, converted to the susceptibility $\chi''(\nu) = S(\nu)/(n(\nu)+1)$, where $n(\nu)$ is the Bose factor. The spectra are normalized to equal integrated intensity of the intense non-polarized Raman band at 44 THz (1466 cm^{-1}) that is due to CH_2 deformations [16]. More specifically and by analogy with vibrational group frequency assignments in chain hydrocarbons, this band is likely due to CH_2 scissor vibrations, which are known to be strongly localized on the CH_2 chemical units and thus fairly independent of the rest of the intra- and inter-molecular structure (viz. Einstein oscillators). In the case of glycerol, the adjacent CH_2 units in a single molecule are separated by two C-C segments (∼2.5 Å), which is sufficiently long a distance to make interactions relatively small. This conclusion is further supported by the absence of any band splitting or frequency shift with temperature. Thus, the 1466 cm^{-1} band intensity is directly proportional to the number of molecules in the scattering volume, so that using it as an intensity reference effectively eliminates the instrumental scatter of the measured intensities at different temperatures, as well as compensates for temperature changes of the density and refractive index.

The spectra in Figure 2a exhibit typical changes of the dynamic susceptibility of a glass former with temperature. At $T \lesssim T_g$ (160 and 180 K), the behavior is almost harmonic (independent of T), the only observable change being a slight variation of the quasielastic intensity at $\nu \lesssim 100$ GHz below the boson peak at ∼1 THz. Above T_g, this excess intensity increases much faster with temperature, at the same time as there appears a minimum at low frequencies, signaling that the tail of the α-relaxation peak enters the explored spectral window. Finally, at high T the α-peak itself appears, eventually approaching the boson peak. Two further apparent features of the spectra are: i) The α-peak intensity decreases with increasing T; ii) the susceptibility minimum flattens with decreasing T but remains in the spectral window even at 190 K, which is a mere few degrees above T_g, even though the α-peak is then expected to have moved by 9 decades into the Hz frequency range. As far as we are aware, it is rather unusual to observe a susceptibility minimum in light scattering spectra close to T_g. One reason is that in many glassformers the minimum will then have moved below ∼300 MHz and thus outside of the accessible frequency range. Another reason, however, is that even if the frequency of the minimum is accessible, its intensity becomes very low at low T, see Figure 2a. A sensitive low-noise detection is thus required. Moreover, it is exactly in this region of very low spectral density that spurious features due to imperfect technique are most likely to appear. We note in this respect that the shape of the susceptibility minima in the light scattering data of Wuttke et al. [7] is rather different from ours. We believe that their data suffered from the "spectral folding" effect discussed above and are therefore not reliable, especially in the vicinity of the susceptibility minimum at low T.

We will now perform quantitative analyses of the spectra and start by determining the temperature dependence of the relaxation time τ_α^{ls} (we shall use superscripts "ls" and "diel" to distinguish depolarized light scattering results from dielectric spectroscopic ones).

3.1 Mean relaxation time

To determine τ_α^{ls}, we fit the high-T spectra that exhibit the α-peak, in the region of the peak, to the Cole-Davidson (CD) function $\mathrm{Im}\,[(1-i\omega\tau_{CD})^{-\beta_{CD}}]$ (see Fig. 3). The mean relaxation time is then $\langle\tau_\alpha\rangle = \tau_{CD}\beta_{CD}$. Figure 4 presents $\langle\tau_\alpha^{ls}\rangle$ together with the dielectric $\langle\tau_\alpha^{diel}\rangle$ of references [1,5]. The peak shape parameter β will be discussed later in Section 3.3. The dashed line is a 4-parameter extended free volume fit from reference [1] to the dielectric data,

$$\log_{10}\langle\tau_\alpha^{diel}\rangle = A + \frac{B}{T - T_{EFV} + \sqrt{(T-T_{EFV})^2 + CT}}, \quad (1)$$

which we reproduce here as a convenient and accurate parameterization of the experimental data. We obtained

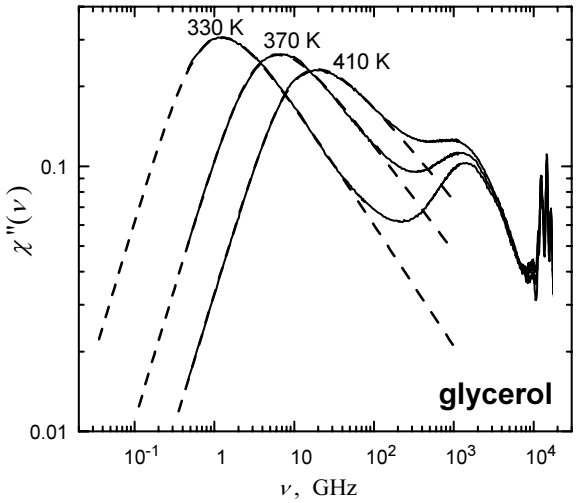

Fig. 3. Sample Cole-Davidson fits (dashed lines) to the spectra of Figure 2, yielding the relaxation time $\langle\tau_\alpha^{ls}\rangle$ (Fig. 4).

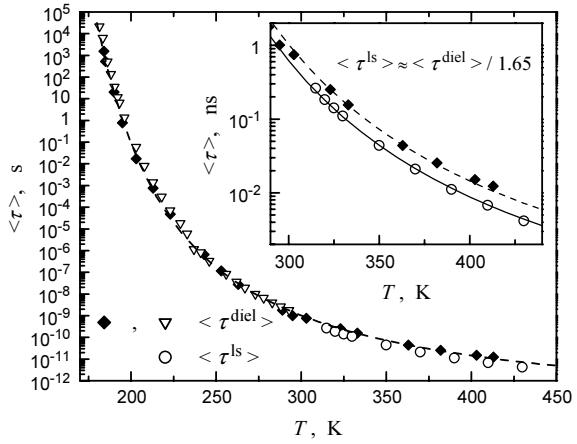

Fig. 4. Mean α-relaxation times from the spectra of Figure 2 (circles) and from the dielectric spectra of reference [1] (diamonds) and [5] (triangles).

the best fit with slightly different parameters than in reference [1], namely $A = -4.687$, $B = 1434$, $T_{EFV} = 152.5$ K, and $C = 10.44$. It is seen that the relaxation times deduced from the light scattering data are somewhat faster than the dielectric ones, but otherwise exhibit the same temperature dependence. This is an expected behavior. Indeed, it is a well-established experimental fact that both relaxation times usually follow the temperature dependence of the viscosity. The insert in Figure 4 shows the high-T part of the data on a smaller scale. The full line was obtained by dividing the fit to the dielectric data (dashed line) by 1.65, so as to achieve the best overlap with the light scattering results. One therefore concludes that $\langle\tau_\alpha^{diel}\rangle \approx 1.65\langle\tau_\alpha^{ls}\rangle$ in the temperature range 315–430 K, where we could extract $\langle\tau_\alpha^{ls}\rangle$. This result that $\langle\tau_\alpha^{ls}\rangle$ is similar to, but somewhat faster than $\langle\tau_\alpha^{diel}\rangle$ is, in our experience, a general property of molecular liquids (we will later illustrate it also for propylene carbonate, see Fig. 10). The reason for such a relation is easy to understand if one recalls that, in first approximation, depolarized light scattering and dielectric relaxation both occur because of molecular reorientations, expressed in terms of the orientational correlation functions of 1st and 2nd rank, respectively [17]:

$$\phi^{diel,ls}(t) = \langle P_{1,2}(\cos\theta_t)\rangle, \tag{2}$$

where $P_l(x)$ is the Legendre polynomial of rank l ($l = 1, 2$), and $\theta_t = \theta(t) - \theta(0)$ the angle through which the molecular axis rotates in time t. Writing out $P_l(x)$ for $l = 1, 2$ we have

$$\phi^{diel}(t) = \langle\cos\theta_t\rangle, \quad \phi^{ls}(t) = \left\langle\left(3\cos^2\theta_t - 1\right)/2\right\rangle. \tag{3}$$

As a rough estimate, $\phi(t)$ decays to 0 when the molecules have rotated by $\sim 90°$ for ϕ^{diel} and by $\sim\arccos(1/\sqrt{3}) = 55°$ for ϕ^{ls}, so that the decay time $\langle\tau_\alpha^{diel}\rangle$ of $\phi^{diel}(t)$ is indeed similar to, but somewhat slower than $\langle\tau_\alpha^{ls}\rangle$ of $\phi^{ls}(t)$. In general, the ratio $\langle\tau_\alpha^{diel}\rangle/\langle\tau_\alpha^{ls}\rangle$ depends on the underlying stochastic process and, if intermolecular correlations are neglected, ranges from 1 for random-angle jump reorientations to 3 for small-step rotational diffusion [17]. We conclude that the ratio of 1.65 that we found for glycerol falls in this range, indeed as one would expect.

3.2 Static susceptibility

At high T, the α-peaks of Figure 2a visibly decrease in intensity with increasing T, and therefore the corresponding static susceptibility

$$\chi_0^{ls} = \frac{2}{\pi}\int_{-\infty}^{+\infty}\chi''(\nu)\, d\ln\nu \tag{4}$$

is temperature dependent. Contrary to the dielectric static susceptibility $\chi_0^{diel} = \epsilon_0 - \epsilon_\infty$, where both the static (ϵ_0) and high frequency (ϵ_∞) dielectric permeability can be measured, the depolarized light scattering susceptibility χ_0^{ls} is not easily accessible experimentally. In order to determine χ_0^{ls}, one therefore has to integrate the experimental spectra, according to equation (4). A technical difficulty is that the experimental spectra do not extend down to $\nu = 0$ as equation (4) requires, and therefore one can only obtain meaningful results when the α-peak is within the experimental frequency window, i.e. at high T. Even then, in order to avoid sizeable truncation errors one has to extrapolate to $\nu = 0$. We extrapolated the spectra at $T = 315$ K through 430 K to low frequencies, using the CD fits of Figure 3, and further to $\nu = 0$ using the physically correct asymptotic behavior $\chi(\nu) \propto \nu$ at $2\pi\nu\tau_\alpha \ll 1$. We then integrated the extended spectra numerically (Eq. (4)) up to $\nu = 10$ THz, retaining thereby only the contributions of molecular reorientation (possibly collective) dynamics, and excluding the high-frequency Raman spectrum of internal molecular vibrations. Figure 5 shows the so-obtained χ_0^{ls} versus T (circles) together with the dielectric susceptibilities from reference [1] (diamonds). χ_0^{ls} data were suitably rescaled to optimize their overlap with the dielectric data. One concludes from Figure 5 that the temperature dependences

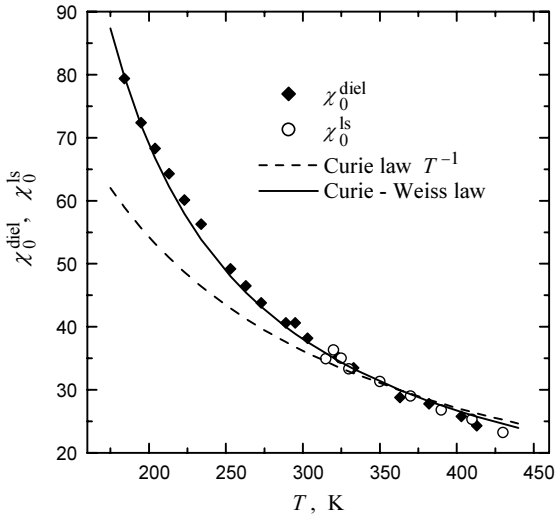

Fig. 5. Temperature dependence of the static susceptibilities (symbols). Broken line is a T^{-1} fit to the data at high $T >$ 300 K. Full line is a fit of the dielectric data to the Curie-Weiss law $(T - T_C)^{-1}$ with Curie's temperature $T_C = 84$ K.

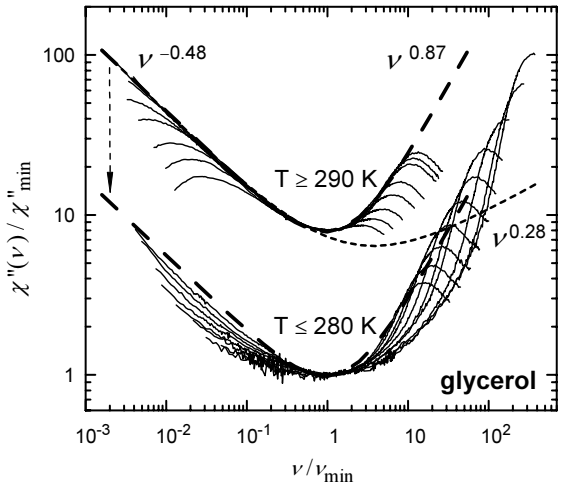

Fig. 6. Susceptibility spectra of Figure 2a, rescaled by the coordinates of their susceptibility minima χ''_{min}, ν_{min} ($T \geq$ 290 K group of spectra shifted up for clarity). Broken lines are two-power-law asymptotic shapes.

of χ_0^{diel} and χ_0^{ls} at high T (where χ_0^{ls} could be obtained) are, to a T-independent factor, identical within experimental scatter. We now proceed to discuss the origin of the temperature dependence of the static susceptibility. The basic (and trivial) temperature dependence of a static susceptibility inversely with the temperature is known, originally concerning only the magnetic susceptibility, as Curie's law. This dependence is typical of a system of uncorrelated molecules, where the macroscopic susceptibility is a sum of single-molecule contributions (see Appendix). It is also the correct high-T limit of $\chi_0(T)$ even in interacting systems, since at $T \to \infty$ the thermal energy overwhelms the intermolecular interaction energy and the molecules do become uncorrelated. In the present case one observes, however, that Curie's law is a poor approximation even at high temperatures (dashed line in Fig. 5), and thus intermolecular interactions play important role even in this temperature range. This is not surprising in view of a high molecular dipole of glycerol and the presence of hydrogen bonds. We notice however that the dielectric data in the whole T-range fit well to the Curie-Weiss law $(T - T_C)^{-1}$ (full line), where T_C is Curie's temperature (not to be confused with the MCT critical temperature T_c). Together with the noted similarity of $\chi_0^{diel}(T)$ and $\chi_0^{ls}(T)$ at high T, this leads us to assume that at low T the light scattering susceptibility can be approximated by the same Curie-Weiss law, too. We realize that, except for the trivial case of Curie's law, different static susceptibilities need not exhibit the same T-dependence (see Appendix). In the present case we base our assumption that $\chi_0^{diel}(T) \propto \chi_0^{ls}(T)$ on the following, somewhat loose argument. Curie-Weiss T-dependence of the dielectric permittivity is usually taken to mean that intermolecular interactions favor the ferroelectric type of dipole ordering. At T_C such interaction would lead to a ferroelectric order-disorder transition, whereby a spontaneous polarization occurs and the dielectric permittivity diverges. At the same time the system becomes aligned and thus turns birefringent, so that $\chi_0^{ls}(T)$ diverges at the same T_C, too. In the case of glycerol the phase transition cannot occur, since $T_C \approx 84$ K and is thus $< T_g$. It is however reasonable to assume that even in the pre-transition temperature range $\chi_0^{diel}(T)$ and $\chi_0^{ls}(T)$ follow similar dependences, especially recalling the experimentally observed similarity at high T. We therefore assume

$$\chi_0^{ls}(T) \propto (T - 84\ \mathrm{K})^{-1} \tag{5}$$

in the whole T-range. In Figure 2b we re-plot the spectra of Figure 2a, dividing out this temperature dependence of χ_0^{ls}. As a result, the apparent α-peak amplitude becomes temperature independent. Indeed, α-relaxation contributes the main part to χ_0. On the other hand, the high-frequency (vibrational) part of the susceptibility in the representation of Figure 2b has acquired an apparent T-dependence, while in fact a harmonic susceptibility is temperature independent. This means that, if χ_0 is T-dependent, it is impossible to normalize the spectra to the same integrated intensity and maintain at the same time the temperature independence of their harmonic parts.

3.3 Temperature evolution of the susceptibility minimum: Phenomenological analysis

The fits in Figure 3 show that the Cole-Davidson function fails to describe the data at frequencies significantly above the α-peak frequency, where the susceptibility goes over through a minimum to a positive slope. As already noted, the shape of the minimum is T-dependent: at low T the minimum becomes flatter. To better illustrate this observation, we re-scale the spectra of Figure 2a so that their minima overlap. In Figure 6 these rescaled spectra are plotted in two groups, $T \leq 280$ K and $T \geq 290$ K.

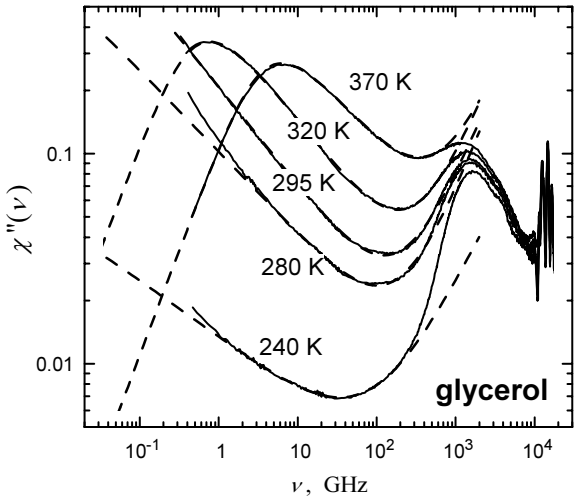

Fig. 7. Sample fits of the susceptibility spectra to the hybrid model, equations (6) and (7).

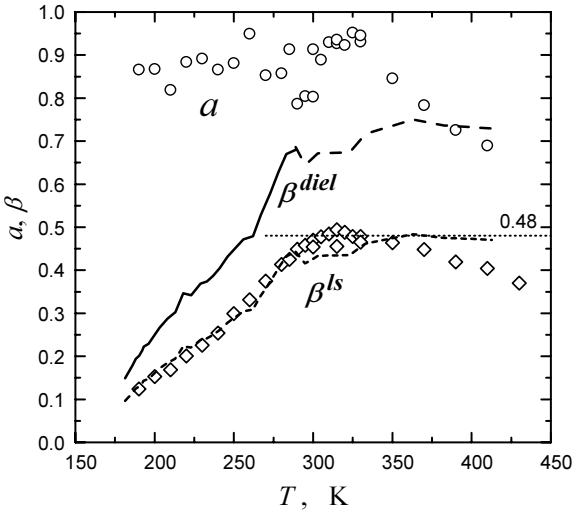

Fig. 8. Symbols are a and β from the hybrid fits of the light scattering spectra (Fig. 7). Full and broken lines represent β^{diel} of the dielectric data. Short-dashed line is $\beta^{diel}/1.5$. Horizontal line shows $\beta = 0.48$, used for the asymptotic shapes of Figure 6.

At $T \geq 290$ K, the spectra around the minimum essentially overlap, falling onto a common "master curve" (dashed line), which means that in this temperature range the shape of the minimum is temperature independent. In contrast, at $T \leq 280$ the curves do not overlap, and the flattening of the minimum is rather apparent. We note that the dielectric loss spectra exhibit qualitatively similar trends.

To quantitatively analyze the shape of the minimum, we use a simple extension of the CD model that includes a power-law additive term ν^a with a positive exponent a. The susceptibility minimum is thus described by a combination of the $\nu^{-\beta}$ tail of the CD function and ν^a. Such "hybrid" model has been utilized in several recent publications on supercooled liquids (see, for example, references [18,19]). The shape of the susceptibility minimum of the hybrid model is formally compatible with the asymptotic results of MCT, even though we will later see that, in the present case of glycerol, the numerical values of the exponents β and a that describe our data turn out to be incompatible with the theory. Following reference [18], we define the "hybrid" function as follows:

$$\chi''(\omega) = \mathrm{Im}\, A\left[(1 - i\omega\tau_\alpha)^{-\beta} + i\omega B\left(\tau_\alpha^{-1} - i\omega\right)^{a-1}\right], \quad (6)$$

where ω is the angular frequency. The second term is a Fourier transform of $t^{-a}\exp -t/\tau_\alpha$; at $\omega \gg \tau_\alpha^{-1}$ its imaginary part is $\propto \omega^a$. At $T \leq 310$ K, where the α-peak is outside of the spectral window, we used a simplified version of equation (6),

$$\chi''(\omega) = A\omega^{-\beta} + C\omega^a, \quad (7)$$

where C is trivially related to A and B of equation (6). Figure 7 shows fits of the hybrid model to our data at selected temperatures. At 295, 320 and 370 K the fitting range was from ∼400 MHz (the lowest studied ν) up to ∼400 GHz, i.e. 3 decades. One observes that the fit quality in this temperature range is excellent, i.e. the hybrid model provides an adequate description of both the α-peak and the minimum. At lower T, starting at about 290 K, we discovered, however, that the values of β that gave satisfactory description of the minimum failed to fit the data at lower ν. We therefore limited the fitting range for $T \leq 290$ K to 1-2 decades about the minimum. Looking at the resulting fits, 240 and 280 K in Figure 7, two things are apparent. First, β of the minimum decreases with decreasing T (i.e. the slope to the left of the minimum decreases), and thus the minimum becomes flatter. Second, at ν significantly below the frequency of the minimum, the slope of the susceptibility goes up, which is why the fit quality there is poor. It thus appears that the tail of the α-peak, which is its only part that remains in the spectral window at low T when the main peak itself has moved way out, is flatter than (goes in excess of) the $\nu^{-\beta}$ flank of the main peak, and that this "excess wing" first becomes detectable in our spectra at $T \sim 290$ K. We note that the excess wing is clearly observed in the dielectric spectra of reference [1] that cover a much wider range of frequencies. The temperature at which it first appears as a discernible feature in the dielectric data, 290 K according to the analysis of reference [12], is also similar to ours.

In the fitting procedure, we first let both a and β vary as free parameters. This resulted in a-values that jumped erratically at different T about the mean of ∼0.87, see circles in Figure 8 (the apparent systematic decrease at high T should not be taken seriously, as the minimum is then almost extinct, and thus the deduced a rather unreliable). We then fixed a at its mean value $a \simeq 0.87$ and repeated the fits. The β-values that were obtained with $a = 0.87$ are presented in Figure 8 as diamonds. Above ∼290 K, β stays almost constant at ∼0.48 and then decreases weakly at $T > 350$ K. At $T \lesssim 290$ K, β decreases rather steeply with decreasing T, which happens, as discussed above, when the main peak has moved out of the spectral window, while its excess wing is starting

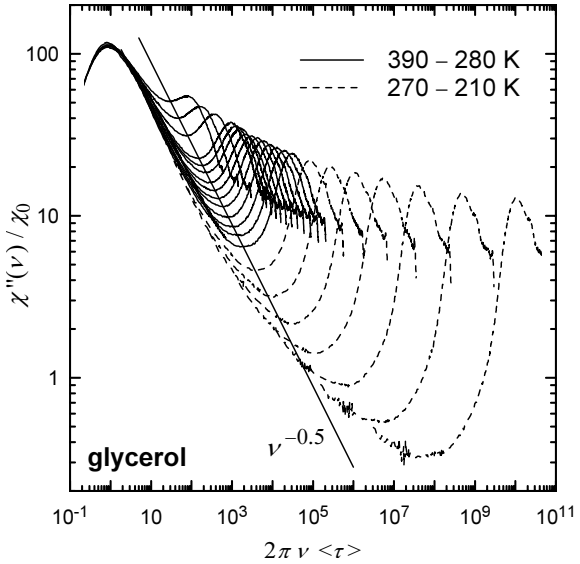

Fig. 9. Susceptibility spectra of Figure 2b plotted versus $2\pi\nu\langle\tau\rangle$, so that their α-peaks overlap.

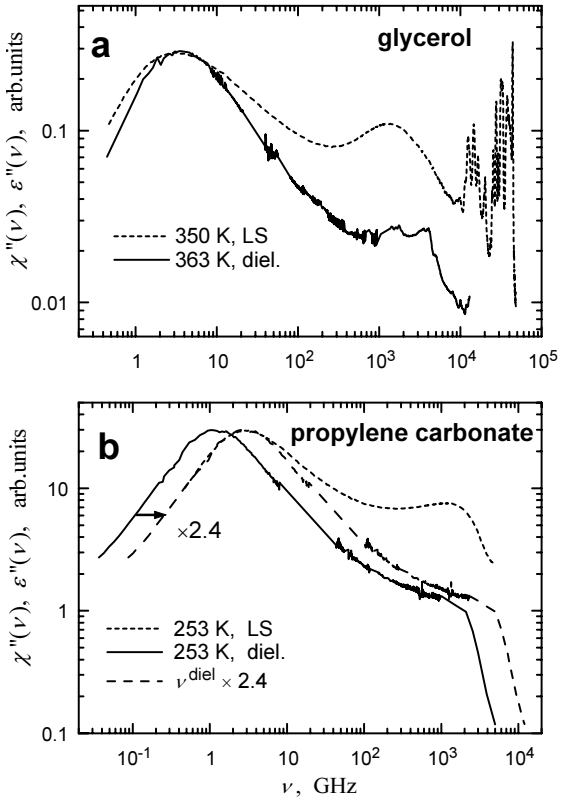

Fig. 10. Comparisons of dielectric loss [1] and depolarized light scattering spectra of glycerol and propylene carbonate.

to emerge. The wing flattens monotonically with decreasing T to a value as low as ∼0.1 below 200 K, which is a behavior also found in the dielectric data [12]. To facilitate further comparisons, we include the dielectric data of the "wing exponent" γ [12] (which is equivalent to our "effective" β at low T) as full line in Figure 8. At higher T we present β from our CD fits to the same dielectric data (broken line). The two lines together thus comprise the dielectric β^{diel} that is equivalent to our light scattering β^{ls} presented by diamonds. The short-dashed line, which is the dielectric data divided by 1.5, is seen to follow closely the light scattering points. Thus, the temperature dependences of β^{diel} and β^{ls} are rather similar, even though β^{diel} is ca. 50% larger. Remarkably, the change in slope of both dependences, which we believe occurs due to the emergence of the "excess wing" at low T, happens at about the same temperature between 290 and 300 K.

As an alternative way to qualitatively analyze the temperature evolution of the susceptibility spectra without resorting to empirical models, we present in Figure 9 the spectra of Figure 2b plotted versus $2\pi\nu\langle\tau_\alpha^{ls}\rangle$, where we assumed $\langle\tau_\alpha^{ls}\rangle \approx \langle\tau_\alpha^{diel}\rangle/1.65$ in the whole T-range (see Sect. 3.1) and used equation (1) for $\langle\tau_\alpha^{diel}\rangle$. In this representation the α-peaks of the spectra at different T overlap. This representation, which was first introduced by Wiedersich et al. [19], provides means to estimate the shape of the peak at low T, when the actual peak is well outside of the experimental window. It also allows to easily distinguish different regimes of temperature evolution of the spectral shape. At high T (full lines), the shape of the α peak and of the minimum is almost T-independent. The minima fall therefore (on the log scale of the figure) on a straight line with approximately the same slope as the high-frequency flank of the peak, as shown in the figure. At low T (broken lines) the minima depart from the straight line, signaling the emergence of the "excess wing" at $2\pi\nu\langle\tau\rangle \gg 1$. It thus appears clear that the excess wing is well pronounced in depolarized light scattering of glycerol and emerges, in a way quite similar to the dielectric data, at $T \lesssim 290$ K. We note though that such a behavior is not a general rule [20].

Next we proceed to directly compare our light scattering data with the published dielectric results. In Figure 10a we present the 350 K light scattering spectrum together with the dielectric loss spectrum [1] at 363 K. The spectra where shifted vertically to match the amplitudes of the peaks. It is immediately clear from the figure that the peak shapes are markedly different: the light scattering peak is much wider (more stretched). Numerically, we find $\beta^{ls} = 0.48$, while $\beta^{diel} = 0.68$ [12]. We note that, to our experience, different shapes of α-peaks in dielectric versus light scattering spectra can often be anticipated from the literature data (see the example of propylene carbonate in Figure 10b), although high-frequency dielectric spectra are not easily accessible and thus direct comparisons are rarely made [1,7]. Apart from a marked difference in the shape of the α-peaks in Figure 10, there is a clear difference in the intensity of the fast dynamics above the peak, which is much stronger in the light scattering data. As a possible explanation of this behavior we note that, from a short-time expansion of the orientational correlation functions and under certain assumptions, the intensity of the depolarized light scattering spectrum above the peak is expected to be 3 times larger than of the

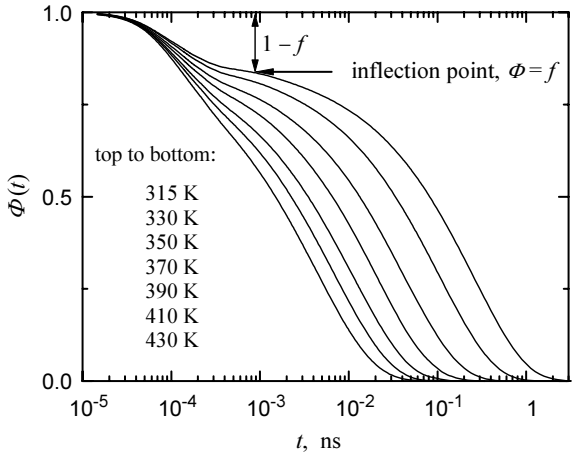

Fig. 11. Normalized correlation functions of glycerol, obtained from the spectra of Figure 2.

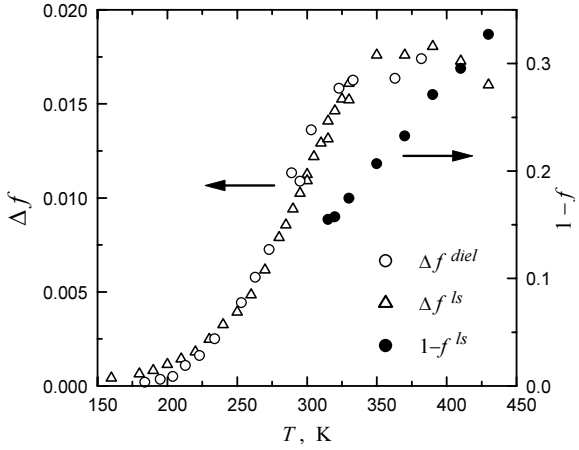

Fig. 12. Non-ergodicity parameter f of the correlation functions of Figure 11, presented as $1 - f$ (filled circles). Strength of the fast relaxation Δf (open symbols), obtained from fits (see text).

dielectric spectrum [20,21]. The ratio χ^{ls}/χ^{diel} at frequencies significantly above the α-peak in Figure 10 is indeed close to 3.

3.4 Non-ergodicity parameter

Among the prominent features of the glass transition one notes the so-called anomaly of the Debye-Waller factor and the closely related temperature dependence of the non-ergodicity parameter f. To remind the reader the meaning of f, let us consider a particle whose "microscopic density" is given by $\delta(\boldsymbol{r} - \boldsymbol{r}_i(t))$. Its correlation function is then, in Gaussian approximation, $\phi(q,t) = \exp(-q^2\langle\Delta r^2(t)\rangle/6)$ [22]. In a solid, the mean square displacement $\langle\Delta r^2(t)\rangle$ is finite at all times, so that the correlation function decays to a finite value f, and in this sense the system is non-ergodic. In a liquid, however, $\langle\Delta r^2(t)\rangle$ increases at long t without limit, so that $\phi(q, t \to \infty) = 0$. Therefore, f as the long-time limit of the correlation function effectively measures the degree of non-ergodicity. It is consequently called "non-ergodicity parameter". In a supercooled liquid, which is a visco-elastic medium, the long-time limit of correlation functions is zero, but the short-time (solid-like) and long-time (diffusive) dynamics are widely separated in time, so that one can generalize the non-ergodicity parameter to mean the value of the intermediate "plateau" of $\phi(t)$ that is reached at $t = t_0$ that separates the fast and slow dynamics. At low $T < T_g$ the dynamics are approximately harmonic, and therefore $\langle\Delta r^2\rangle \propto T$. Since $f = \exp(-q^2\langle\Delta r^2\rangle/6) \approx 1 - q^2\langle\Delta r^2\rangle/6$, it follows that $1 - f \propto T$. At $T > T_g$ the experimental $1 - f(T)$ increases, however, steeper than linear, which constitutes the mentioned anomaly. At $T = T_c$, MCT predicts a singularity of $f(T)$ with T-independent behavior above T_c. It was this prediction that triggered renewed interest in the non-ergodicity parameter and its temperature dependence in the past two decades. Non-ergodicity parameters of correlation functions other than the density-density correlator, such as orientational correlations relevant in dielectric and depolarized light scattering spectroscopy, are defined in the same manner and presumably have similar T-dependences.

Figure 11 presents normalized ($\phi(0) = 1$) correlation functions that were obtained by numerically computing the Fourier transform of the high-temperature spectra of Figure 2b extrapolated to $\nu = 0$ as discussed in Section 3.2. The Raman spectrum of internal molecular vibrations above 10 GHz was not included in the transform. At $T < 315$ K, when the α-peak is outside of the explored frequency window, the low-ν truncation does not allow a reliable estimation of $\phi(t)$. At high T, the correlation functions of Figure 11 lack well-defined plateaus, so that f cannot be simply read off the graph. Instead of a plateau, it is more appropriate to consider the inflection point of $\phi(\log t)$, so that f is equal to $\phi(t)$ at the inflection point. We therefore analyzed $\phi(t)$ of Figure 11 numerically to find their inflection points. The values of $1 - f$ that we found from this analysis are presented by filled circles in Figure 12. One observes that $1 - f(T)$ increases steadily, which is reminiscent of the low-T behavior $1 - f(T) \propto T$, and that there is no sign of a T-independent $1 - f$, as one would expects from MCT. This is not surprising in view of the fact that the major contribution to $1 - f$ comes from the boson peak, and that the latter is only weakly T-dependent even at high T, see Figure 2a. As already discussed, an approximately T-independent (quasi-harmonic) behavior of the fast dynamics (boson peak) translates into $\propto T$ underlying dependence of $1 - f$. We note in this respect that, even though the MCT equation of motion for the density correlation function is an oscillator equation, its non-trivial solutions only occur in the limit of strong coupling of the density modes, and thus ignore the short-time oscillatory behavior in more realistic quasi-harmonic potentials.

Instead of analyzing $1 - f(T)$, whose main T-dependence is rather trivial, one can try to single out the contribution of the fast relaxation dynamics Δf to $1 - f$, i.e. to estimate the strength of these dynamics. If the dynamics were purely relaxational, then Δf would

have the same meaning as $1 - f$. Such an approach requires of course a model for the dynamics. We have seen that empirically the minimum is well accounted for by introducing a power-law term ν^a, and thus the amplitude of this term may be used as a measure of Δf. One can furthermore use the integrated intensity of the ν^a term from fits to normalized (total area =1) spectra, and thereby put Δf on the absolute scale. Using this procedure, Δf was estimated in reference [12] from dielectric spectra, where the authors also claimed that their estimates were in absolute units. One has to note in this respect that ν^a (viz. ω^a of Eq. (6)) as a model of the fast relaxation dynamics is unphysical in both low- and high-ν limits. At $\nu \to 0$ and $a < 1$, it leads to a diverging spectral density, while no such divergence is observed in practice (we note that the hybrid function of Eq. (6) is constructed to remove this divergence). At high frequencies, ν^a increases without limit, while in reality the relaxation spectrum merges with the boson peak. In the estimation of Δf of reference [12], the authors ignored the first issue and circumvented the second by limiting the integration range to 200 GHz. We literally followed this prescription for our light scattering data in order to extract Δf that can be compared with the dielectric results of reference [12]. More specifically, we computed $\Delta f = (1/\chi_0^{ls}) \int_{-\infty}^{\ln \nu_{max}} C\nu^a \, d\ln\nu$, where $\nu_{max} = 200$ GHz, C and $a = 0.87$ were obtained from the hybrid fits (see Sect. 3.3), and χ_0^{ls} is the static susceptibility, equation (5). The so-obtained $\Delta f(T)$ are presented in Figure 12 together with the corresponding dielectric results of reference [12]. One immediately observes that the temperature dependences of Δf^{ls} and Δf^{diel} are remarkably similar, including even their numerical values. The latter observation should not however be literally taken to mean that the fast relaxation dynamics has the same amplitude in depolarized light scattering and dielectric spectra, since the numerical values of Δf, obtained as described above, depend strongly on the values of the exponent a that were rather different in their fits of the dielectric data ($a = 0.337$) and our light scattering fits ($a = 0.87$). Recalling the comparisons of Figure 10 and the related discussion in the end of Section 3.3, one should rather conclude that $\Delta f^{ls} > \Delta f^{diel}$, perhaps $\Delta f^{ls}/\Delta f^{diel} \sim 3$. The similarity of the temperature dependences is reassuring, as it suggests that it is the same underlying fast relaxation dynamics that is associated with the susceptibility minimum of both the light scattering and dielectric spectra. One further notices that $\Delta f(T)$ exhibits rather different behavior at low and high temperatures. At $T \lesssim 320$ K, Δf^{ls} increases steeply with T, while above 320 K it stays almost constant. This is reminiscent of the high-T prediction of MCT for the non-ergodicity parameter. Based on that, we can take 320 K as the MCT critical temperature. Such estimate of T_c is then substantially higher that any previously reported, see Section 1. We will however show in Section 3.5 that the overall shape and temperature evolution of our spectra do not allow any numerical MCT analyses. But we also cautiously note that at high T, where the thermal energy becomes significantly larger than the H-bonding energy, the tensorial and harmonic parts of intermolecular interactions become less important, and the liquid starts to resemble a system of hard spheres. It may explain why Δf exhibits an MCT-like (T-independent) behavior at high T, even though the spectra on the whole are rather incompatible with the theory.

3.5 Is MCT applicable?

Turning now to the possibility of an MCT analysis of our data, possibly for the purpose of extracting T_c, we immediately note that the shape of our susceptibility minima is incompatible with the asymptotic laws of the theory. We recall that the minimum in MCT is asymptotically described with a combination of two power laws $\nu^{-\beta}$ and ν^a (MCT literature commonly uses b in place of β), which is equivalent to our extrapolation. However, a larger than 0.395 is impossible in the theory, provided that $b \leq 1$, while we find $a \sim 0.87$ at all temperatures.

We now recall that in all known MCT models the so-called critical exponent λ ($1/2 < \lambda < 1$) is independent of the particular probing variable, as long as the latter couples to the density fluctuations. Since, within the theory, both a and β of the minimum are determined by λ through $\lambda = \Gamma^2(1-a)/\Gamma(1-2a) = \Gamma^2(1+\beta)/\Gamma(1+2\beta)$ ($\Gamma(x)$ is the gamma function), it means that a and β should be the same for different susceptibilities. Inspection of Figure 10a reveals that this is certainly not the case in glycerol: the slope to the left of the minimum (β) of the dielectric data is clearly steeper than in the light scattering spectra. Numerically, $\beta^{ls} = 0.48$, while $\beta^{diel} = 0.68$ (Sect. 3.3). To our experience, a similar difference of the spectral shapes, although less pronounced, is typical of molecular glass-formers, see Figure 10b for the example of propylene carbonate.

The values of a^{ls} and a^{diel} cannot be compared, since the dielectric minimum is not well pronounced, and thus a^{diel} is poorly defined. On the other hand, this leaves more freedom in fitting procedures of the dielectric data. For instance, in the asymptotic MCT analysis of the dielectric data in reference [12], the authors constrained $a = 0.34$ so as to comply with the MCT restriction that follows from $\beta^{diel} = 0.68$ and were able to fit the data with this constraint. In the case of our light scattering data, the minimum is well pronounced, which leaves no room for using spurious constraints. In particular, $\beta^{ls} = 0.48$ implies, according to MCT, $a^{ls} = 0.28$. This is shown by short-dashed line in Figure 6. It is completely clear that with such a constraint it is impossible to obtain reasonable fits to our data. The data are thus incompatible with the asymptotic scaling laws of the theory.

One can however argue that the scaling laws are a leading order asymptotic result whose range of validity may be rather limited, and that one should instead compare the experimental data with full solutions of an MCT model. Such analysis was reported in reference [23], where the so-called two correlator schematic model of MCT was used to analyze neutron, light, and dielectric spectra of propylene

carbonate. The authors of reference [23] were able to simultaneously fit all the three datasets with full solutions of the model. Then they analyzed how well the asymptotic laws were fulfilled for the solutions and found a reasonable agreement. They argued however that the scaling laws alone were insufficient to properly analyze the data. We note in this respect that the asymptotic laws, albeit obviously limited in validity, are the only generic theoretical prediction of the properties of the susceptibility spectra. Using two-correlator, or more elaborate models with sufficiently many adjustable parameters apparently gives enough flexibility in fitting experimental data, especially if the susceptibility minimum is poorly pronounced and/or obstructed by experimental noise, such as in the mentioned data of propylene carbonate. Interestingly, MCT solutions for rotational dynamics of a guest elongated molecule in a hard sphere liquid correctly reproduce the different α-peak stretching of the orientational correlation functions of first and second rank [24,25], which appears to imply that the stretching exponent of the peak is then different from the asymptotic exponent of the minimum.

Turning now to the non-ergodicity parameter f and its theoretically expected critical temperature dependence, no such critical dependence could be identified in the temperature range $T \gtrsim 310$ K, see filled circles in Figure 12. Extracting, however, the relaxational part Δf of $1 - f$ yields a temperature dependence with an apparent break at 300–320 K (open symbols in Fig. 12), which may be identified with T_c. As a note of caution, there is to our knowledge no model-independent way to extract Δf; the results are therefore biased. Then, such an estimate of T_c is higher than any other reported so far. In particular, it is almost 100 K higher than in the comprehensive MCT analysis of reference [10].

4 Conclusions

We obtained depolarized light scattering spectra of the classic glass former glycerol, taking the necessary precautions to avoid experimental artefacts. We believe, in particular, that our data do not suffer from the "spectral folding" effect, which is a known source of errors in interferometric spectroscopy of continuous spectral sources.

Overall, the susceptibility spectra exhibit a typical shape and temperature dependence of a glass former. Their particularity, however, is the presence of a minimum in the explored frequency window ($\geq$400 MHz) down to T_g and flattening of the minimum with decreasing the temperature below ca. 280–290 K. We show that both effects are due to the emergence and temperature evolution of the "excess wing" in a way quite similar to its manifestation in dielectric loss spectra. The excess wing is thus strongly pronounced in depolarized scattering of glycerol. This does not seem, however, to be a general rule. Indeed, photon correlation spectroscopy of picoline, dimethylphthalate, and salol show that in these liquids the wing in depolarized light scattering is either undetectable or weak, contrary to the dielectric loss spectra [20]. This may explain why the excess wing has so far not been unambiguously identified in light scattering.

We find that the integrated spectral density (static susceptibility) is temperature dependent, again in a way quite similar to the corresponding dielectric permittivity. Both have thus a common origin, which we believe to be the underlying T^{-1} dependence of a single-particle response (Curie's law) modified by intermolecular interactions, resulting in an almost Curie-Weiss temperature dependence.

There are important differences between the light scattering and dielectric responses of glycerol. Firstly, the spectrum above the susceptibility minimum ("fast dynamics") is several times more intense in the light scattering than in the dielectric spectra. This may be explained by the corresponding difference between the first and second rank orientational correlation functions [20]. Secondly, the α-relaxation peak is significantly wider in light scattering: the stretching parameter β^{ls} is about 50% larger than β^{diel}. To our knowledge, a different width of dielectric and light scattering relaxation peaks is a rather common phenomenon (cf. Fig. 10b of propylene carbonate), however rarely with such a magnitude. Consequently, the shape of the susceptibility minimum is also rather different.

We find that the shape of the susceptibility minimum is incompatible with the generic asymptotic laws of MCT. Furthermore, the mentioned difference in the shapes of light scattering and dielectric responses is also at odds with the theory. We therefore did not conduct any MCT analysis of our data and believe that such an analysis would be impossible. However, the temperature dependence of the magnitude of the fast relaxation dynamics, related to the non-ergodicity parameter, does flatten out at high T, as theoretically expected. Taken out of context, this would yield the MCT critical temperature within $\sim$300–320 K, which is close to the result $\sim$300 K of the similar dielectric study [12].

Apart from the mentioned differences between the light and dielectric spectroscopic data, there are also clear similarities, as one indeed expects for the techniques that probe the same molecular dynamics. The temperature evolution of both the light scattering and the dielectric loss spectra is qualitatively different at high and low temperatures, so that one can distinguish two temperature regimes. The high-T regime, above $\sim$320 K, is characterized by a nearly T-independent shape of the α-peak and susceptibility minimum, and a nearly T-independent strength of the fast relaxation Δf. The low-T regime below $\sim$280 K is characterized by the emergence of the excess wing and a strong temperature dependence of Δf.

5 Appendix

5.1 Curie law

In discussing the temperature dependence of the static dielectric constant (permittivity) of a dipolar fluid, it is customary to refer to Curie's law $\epsilon_0 \propto 1/T$ as the basic source of the T-dependence. Derivations of Curie's law

are normally couched in terms of a competition between the dipole-aligning influence of the external field and the randomizing influence of thermal motion. In this sense, the law concerns only the orientational polarizability. We will now proceed to show that the variation of a static susceptibility inversely with the temperature is a natural property of any single particle (incoherent) response function of a fluid, in particular of χ_0^{ls} introduced above, insofar as different molecules are uncorrelated.

In the following we will assume a fluid of anisotropic molecules with the number density N. It is convenient to introduce the generalized microscopic density, which explicitly includes molecular orientations Ω_j in addition to the positions in space $\boldsymbol{r}$,

$$\rho(\boldsymbol{r},\Omega)=\sum_{j=1}^{N}\delta(\boldsymbol{r}-\boldsymbol{r}_j)\delta(\Omega-\Omega_j), \tag{8}$$

and expand it in plane waves (Laplace transform) and spherical harmonics [26]:

$$\rho_{lm}(\boldsymbol{q})=\sum_{j=1}^{N}e^{i\boldsymbol{q}\boldsymbol{r_j}}Y_{lm}(\Omega_j). \tag{9}$$

The static correlation function $\langle\rho^*\rho\rangle$ in the limit $\boldsymbol{q}\to 0$ is then

$$\begin{aligned}S_{lm,l'm'}&=\langle\rho^*_{lm}\rho_{l'm'}\rangle=\sum_{j,j'}\langle Y^*_{lm}(\Omega_j)Y_{l'm'}(\Omega_{j'})\rangle\\&=\sum_{j}\langle Y^*_{lm}(\Omega_j)Y_{l'm'}(\Omega_j)\rangle+\sum_{j\neq j'}\langle Y^*_{lm}(\Omega_j)Y_{l'm'}(\Omega_{j'})\rangle.\end{aligned} \tag{10}$$

Neglecting intermolecular correlations (the last term in Eq. (10)) and using $\langle Y^*_{lm}(\Omega_j)Y_{l'm'}(\Omega_j)\rangle=\delta_{ll'}\delta_{mm'}$, we get:

$$S^0_{lm,l'm'}=S^0_l=N. \tag{11}$$

Thus, the static correlation functions of different rank l are simply equal to the number density, under the assumption of the absence of intermolecular correlations. We now recall that the fluctuation-dissipation theorem relates the (time dependent) correlation functions $S(t)$ to the corresponding relaxation (step response) functions $R(t)$ as $S(t)=k_BTR(t)$ and that the same relation naturally holds for the initial ($t=0$) values. Recalling further that the static susceptibility χ_0 is equal to the initial value of the step response function $R(t=0)$, we obtain

$$\chi_0=S^0_l/k_BT=N/k_BT\propto 1/T, \tag{12}$$

which is the familiar Curie law. Thus, if the dipolar ($l=1$) susceptibility exhibits $\chi_0^{diel}\propto 1/T$, then a) it is a good indication of the lack of intermolecular correlations, and b) the higher order susceptibilities (e.g. with $l=2$ for depolarized light scattering) will exhibit this temperature dependence, too. We note in passing that a temperature-dependent behavior of depolarized light scattering integrated intensities can be anticipated from many published studies, although it is rarely given proper interpretation.

5.2 Kirkwood correlation factors

Correlation functions of different ranks are, in general, differently affected by intermolecular correlations, and therefore their temperature dependences may no longer be simply related. Intermolecular correlations can be formally accounted for, using the so-called Kirkwood correlation factors g_l [27]:

$$g_l=\sum_{j=1}^{N}\langle P_l(\boldsymbol{u}_i\cdot\boldsymbol{u}_j)\rangle, \tag{13}$$

where $P_l(x)$ is the Legendre polynomial of rank l ($l=1$ for dielectric and $l=2$ for depolarized light scattering properties). The static susceptibility χ_0^{corr} that includes the effects of intermolecular correlations is then

$$\chi_0^{corr}=g_l\chi_0, \tag{14}$$

where χ_0 is the susceptibility in the absence of correlations, given by equation (12). Thus, $g_l=1$ in the absence of correlations. We note that the effects of correlations may be rather different for the dielectric and light scattering susceptibility, which is best understood by considering simple examples. For instance, if intermolecular interactions favor anti-parallel arrangement of dipoles, then χ_0^{diel} is decreased ($P_1(\cos 180^\circ)=-1$), while χ_0^{ls} is instead enhanced ($P_2(\cos 180^\circ)=+1$). If the molecules preferably arrange orthogonal to each other, then χ_0^{diel} is unaffected ($P_1(\cos 90^\circ)=0$), while χ_0^{ls} is decreased ($P_2(\cos 90^\circ)=-1/2$).

References

1. P. Lunkenheimer, U. Schneider, R. Brand, A. Loidl, Contemp. Phys. **41**, 15 (2000)
2. N. Menon, K.P. O'Brien, P.K. Dixon, L. Wu, S.R. Nagel, J.P. Carini, B.D. Williams, J. Non-Cryst. Solids **141**, 61 (1992)
3. A. Hofmann, F. Kremer, E.W. Fischer, A. Schönhals, in *Disorder Effects on Relaxational Processes*, edited by R. Richert, A. Blumen (Springer, Berlin, 1994), p. 309
4. A. Kudlik, S. Benkhof, T. Blochowicz, C. Tschirwitz, E. Rössler, J. Mol. Struct. **479**, 201 (1999)
5. T. Blochowicz, C. Tschirwitz, S. Benkhof, E.A. Rössler, J. Chem. Phys. **118**, 7544 (2003)
6. W. Götze, L. Sjögren, Rep. Prog. Phys. **55**, 241 (1992)
7. J. Wuttke, J. Hernadez, G. Coddens, H.Z. Cummins, F. Fujara, W. Petry, H. Sillescu, Phys. Rev. Lett. **72**, 3052 (1994)
8. E. Rössler, A.P. Sokolov, A. Kisliuk, D. Quitmann, Phys. Rev. B **49**, 14967 (1994)
9. P. Lunkenheimer, A. Pimenov, M. Dressel, Yu.G. Goncharov, R. Böhmer, A. Loidl, Phys. Rev. Lett. **77**, 318 (1996)
10. T. Franosch, W. Götze, M.R. Mayr, A.P. Singh, Phys. Rev. E **55**, 3183 (1997)
11. W. Götze, J. Phys.: Condens. Matter **11**, A1 (1999)

12. S. Adichtchev, T. Blochowicz, C. Tschirwitz, V.N. Novikov, E.A. Rössler, Phys. Rev. E **68**, 011504 (2003)
13. N.V. Surovtsev, J.A.H. Wiedersich, N.V. Novikov, E. Rössler, A.P. Sokolov, Phys. Rev. B **58**, 14888 (1998)
14. H.C. Barshilia, G. Li, G.Q. Shen, H.Z. Cummins, Phys. Rev. E **59**, 5625 (1999)
15. Sample kindly supplied by A.P. Sokolov (University of Akron, Department of Polymer Science, Akron, Ohio)
16. E. Mendelovici, R.L. Frost, T. Kloprogge, J. Raman Spectrosc. **31**, 1121 (2000)
17. B.J. Berne, R. Pecora, *Dynamic Light Scattering* (Wiley, New York, 1976)
18. A. Brodin, M. Frank, S. Wiebel, G. Shen, J. Wuttke, H.Z. Cummins, Phys. Rev. E **65**, 051503 (2002)
19. J. Wiedersich, N.V. Surovtsev, E. Rossler, J. Chem. Phys. **113**, 1143 (2000)
20. A. Brodin, R. Bergman, J. Mattsson, E.A. Rössler, Eur. Phys. J. B **36**, 349 (2003)
21. T. Blochowicz, A. Kudlik, S. Benkhof, J. Senker, E. Rössler, G. Hinze, J. Chem. Phys. **110**, 12011 (1999)
22. S.W. Lovesey, *Theory of Neutron Scattering from Condensed Matter*, Vol. 1 (Oxford, New York, 1984)
23. W. Götze, Th. Voigtmann, Phys. Rev. E **61**, 4133 (2000)
24. W. Götze, A.P. Singh, Th. Voigtmann, Phys. Rev. E **61**, 6934 (2000)
25. S.-H. Chong, W. Götze, A.P. Singh, Phys. Rev. E **63**, 011206 (2000)
26. C.G. Gray, K.E. Gubbins, *Theory of molecular fluids*, Vol. 1 (Oxford, New York, 1984)
27. C.J.F. Böttcher, P. Bordewijk, *Theory of Electric Polarization* (Elsevier, Amsterdam, 1978)